

# Resonances in a trapped 3D Bose–Einstein condensate under periodically varying atomic scattering length

Fatkhulla Kh Abdullaev<sup>1</sup>, Ravil M Galimzyanov<sup>1</sup>, Marijana Brtko<sup>2</sup>  
and Roberto A Kraenkel<sup>2</sup>

<sup>1</sup> Physical-Technical Institute of the Academy of Sciences, 700084, Tashkent-84,  
G Mavlyanov str., 2-b, Uzbekistan

<sup>2</sup> Instituto de Física Teórica, UNESP, Rua Pumplona 145, 01405-900, Sao Paulo, Brazil

E-mail: ravil@uzsci.net

Received 24 May 2004

Published 24 August 2004

Online at [stacks.iop.org/JPhysB/37/3535](http://stacks.iop.org/JPhysB/37/3535)

doi:10.1088/0953-4075/37/17/009

## Abstract

Nonlinear oscillations of a 3D radial symmetric Bose–Einstein condensate under periodic variation in time of the atomic scattering length have been studied. The time-dependent variational approach is used for the analysis of the characteristics of nonlinear resonances in the oscillations of the condensate. The bistability in oscillations of the BEC width is investigated. The dependence of the BEC collapse threshold on the drive amplitude and parameters of the condensate and trap is found. Predictions of the theory are confirmed by numerical simulations of the full Gross–Pitaevskii equation.

## 1. Introduction

Investigation of collective excitations of a Bose–Einstein condensate (BEC) has attracted considerable attention in recent years [1]. Among the problems of these studies, the dynamical response of the condensate to temporal perturbations in it as a whole is of natural interest. Many efforts have been devoted to the analysis of the effect of temporal modulations of a trap potential on oscillations of the condensate. The parametric and nonlinear resonances in BEC oscillations have been studied in [2–4]. The dynamics of the BEC under rapid strong perturbations of the trap potential has been considered in [5, 6], where the stabilization of the condensate is shown to exist. Since the dynamics is nonlinear, chaotic oscillations are also possible. Recently excitations of multimode dynamics and stochastization in two component condensate oscillations were observed experimentally in [7]. The collapse induced by the noise in the trap has been studied in [8].

It should be noted that the effects of temporal modulations of a trap potential on the condensate and noncondensate parts of the cloud are similar. Interesting nontrivial dynamics of the condensate is also observed under temporal variation of the atomic scattering length by

means of the Feshbach resonances [9]. Distinct from the trap modulations, such variations affect the condensed and thermal parts of an atomic cloud differently. The dynamics of the condensate is governed by the Gross–Pitaevskii equation with varying in time nonlinear term. The temporal modulations of a trap potential lead to the appearance of a *time-dependent linear potential* in the nonlinear Schrödinger equation. The modulation of the scattering length,  $a_s$ , leads to the Schrödinger equation with a *time-dependent nonlinear potential* that opens a new interesting area in the matter waves theory. Here we can mention the Bose–Einstein condensation phenomenon occurring under rapid change of the scattering length value from positive (corresponding to repulsion between atoms) to negative (corresponding to attraction between atoms) [10].

Periodic variation in time of the scattering length causes the appearance of new effects. One of them is pattern formation in 2D BEC [11] (see related 1D problem in the context of nonlinear optics [12]). Another interesting phenomenon is the existence of resonances in the macroscopic quantum tunnelling between two tunnel-coupled condensates [13]. A possible dynamical stabilization of 2D BEC under rapid periodic variation of the atomic scattering length [14, 15] and existence of Feshbach resonances should also be mentioned. Collective oscillations of a 1D Bose–Einstein gas under different external perturbations of the trap and the scattering length have been considered in [16].

Oscillations of 2D BEC have been studied variationally and numerically in [17]. Numerical study of the 3D BEC oscillations has been given in [18]. At the same time analytical consideration of oscillations of 3D BEC is still lacking. A free attractive 3D BEC is known to collapse at any number of atoms. The existence of a trap leads to another situation. For a given trap potential, a 3D BEC collapses if the number of atoms exceeds some critical value. This has been checked experimentally in [19].

The purpose of this work is to investigate variationally and numerically nonlinear oscillations of the 3D radial symmetric BEC under periodic variations of the atomic scattering length. We will employ the time-dependent variational approach and derive a nonlinear ordinary differential equation (ODE) for evolution of the condensate width. We will compare predictions for nonlinear resonances and instability of a condensate with numerical simulations of the full time-dependent Gross–Pitaevskii (GP) equation.

The paper is organized as follows. In section 2, we derive the variational model to describe a 3D Bose–Einstein condensate in a trap potential. In section 3, based on the Van-Der-Pole method, necessary equations are derived to describe main and parametric resonances. In section 4, numerical simulations as well as their analysis are given and finally in section 5 the main results are summarized.

## 2. Variational model

The total wavefunction for a 3D Bose–Einstein condensate in a trap potential  $V_{\text{tr}}(r)$  may be described by the Gross–Pitaevskii equation:

$$i\hbar\Psi_t = -\frac{\hbar^2}{2m}\Delta\Psi + V_{\text{tr}}(r)\Psi + g(t)|\Psi|^2\Psi. \quad (1)$$

Here  $V_{\text{tr}}(r) = m\omega^2 r^2/2$  is a trap potential, the factor  $g(t) = 4\pi\hbar^2 a_s/m$  and  $a_s$  is the atomic scattering length. This GP equation is based on the assumption that the interaction term is determined only by the atomic scattering length for systems with a Feshbach resonance (see e.g. [20] and references therein). We will suppose that the time-dependent scattering length  $a_s$  is constant to leading order, with

$$a_s = a_0\sigma(1 + h \sin(\Omega't)), \quad (2)$$

where  $\sigma$  stands for the dimensionless scattering length.

Such variation can be obtained using for example varying in time magnetic field near a Feshbach resonance [21]. So the atomic scattering length can be expressed as

$$a_s(t) = a_B \left( 1 + \frac{\Delta}{B_0 - B_1(t)} \right), \quad (3)$$

where  $a_B$  is the asymptotic value of  $a_s$  and the magnetic field  $B_1 = B_2 \sin \Omega t$ . Then far from the resonance, we can approximate  $a_s(t) = a_{s0} \sigma (1 + h \sin(\Omega t))$ , with

$$a_{s0} = a_B \left( 1 + \frac{\Delta}{B_0} \right), \quad h = \frac{a_B \Delta B_2}{B_0^2 \left( 1 + \frac{\Delta}{B_0} \right)}.$$

Regarding experimental values of the parameters  $B_0$  and  $\Delta$ , Feshbach resonances have been observed in Na at 853 and 907 G [21], in  $^7\text{Li}$  at 725 G [22] and in  $^{85}\text{Rb}$  at 164 G with  $\Delta = 11$  G [23]. Another way of making variations in the nonlinear term is to vary the tight confined potential parameters of the low-dimensional system. For a 2D pancake BEC it may be the frequency of the trap in the direction of tightening and the transverse trap frequency in the case of a 1D cigar-shaped BEC.

Under the scaling  $\tau = t\omega$ ,  $\rho = r/l_0$ ,  $l_0 = \sqrt{\frac{\hbar}{m\omega}}$ ,  $U = \Psi \sqrt{4\pi a_s l_0^2}$ , the Gross–Pitaevskii equation can be written in the dimensionless form

$$iU_\tau + \frac{1}{2}\Delta U - \frac{\rho^2}{2}U + \sigma(1 + h \sin(\Omega\tau))|U|^2U = 0, \quad (4)$$

where  $\Omega = \Omega'/\omega$  and  $\sigma = 1, \sigma = -1$  corresponds to attractive or repulsive interactions between atoms in the condensate respectively.

For the radially symmetrical case the governing equation takes the form

$$iU_\tau + \frac{1}{2}U_{\rho\rho} + \frac{1}{\rho}U_\rho - \frac{r^2}{2}U + \sigma(1 + h \sin(\Omega\tau))|U|^2U = 0. \quad (5)$$

Corresponding Lagrangian density is determined by the following expression:

$$L(U, U^*) = \frac{i}{2}(U^*U_\tau - UU^*_\tau) - \frac{1}{2}|U_\rho|^2 - \frac{1}{2}\rho^2|U|^2 + \frac{\sigma}{2}(1 + h \sin(\Omega\tau))|U|^4. \quad (6)$$

In deriving our variational model we proceed from the ansatz that the modulus of the total wavefunction,  $|U|$ , evolves in a self-similar way. So a trial function may be taken in the form

$$U(\rho, \tau) = A(\tau)R\left(\frac{\rho}{a(\tau)}\right)\exp\left(i\frac{b(\tau)\rho^2}{2a(\tau)} + i\phi(\tau)\right), \quad (7)$$

where the function  $R^2\left(\frac{\rho}{a(0)}\right)$  describes initial BEC density distribution.

To obtain equations for the wave packet parameters  $A(\tau)$ ,  $a(\tau)$ ,  $b(\tau)$ ,  $\phi(\tau)$ , we calculate the averaged Lagrangian  $\bar{L}(\tau) = \int d^3\rho L(U(\rho, \tau), U^*(\rho, \tau))$  with the trial function (7). Its explicit expression takes the form

$$\bar{L} = -\frac{A^2 a^3}{2} \left( (b_\tau a - a_\tau b + a^2 + b^2)I_2 + 2\phi_\tau n + \frac{I_4}{a^2} - \sigma(1 + h \sin(\Omega\tau))A^2 I_3 \right). \quad (8)$$

Hereafter the following designations for the constants  $n = \int R(\rho)^2 \rho^2 d\rho$ ,  $I_2 = \int R(\rho)^2 \rho^4 d\rho$ ,  $I_3 = \int R(\rho)^4 \rho^2 d\rho$  and  $I_4 = \int R_\rho(\rho)^2 \rho^2 d\rho$  will be used.

The Euler–Lagrange equations for the functional  $\bar{L}(\tau)$  lead to the following equations for the scaling parameter  $a(\tau)$  and chirp  $b(\tau)$ :

$$a_\tau = b, \quad b_\tau = \frac{I_4}{I_2 a^3} - a - \frac{3\sigma(1 + h \sin(\Omega\tau))A^2 a^3 I_3}{2a^4 I_2}. \quad (9)$$

Eliminating the parameter  $b$  from the above system and making substitution  $a = \left(\frac{I_4}{I_2}\right)^{\frac{1}{4}}v$ , we get the following evolution equation for  $v$ :

$$v_{\tau\tau} = \frac{1}{v^3} - v - \frac{\sigma P(t)}{v^4}, \quad (10)$$

where

$$P(\tau) = P_0 + P_1 \sin(\Omega\tau), \quad P_0 = \frac{3\sigma N_1 I_3 I_2^{\frac{1}{4}}}{2n I_4^{\frac{5}{4}}}, \quad P_1 = P_0 h \quad (11)$$

and the quantity

$$N_1 = \frac{1}{4\pi} \int d^3\mathbf{r} |U|^2 = A^2 v^3 \int r^2 dr R^2 = A^2 v^3 n = \frac{N a_s}{l_0}, \quad (12)$$

determines the norm of the wavefunction  $U$ .

It is easy to see that the above is a Hamiltonian system, with the scaling parameter  $v$  playing the role of a position variable, and the chirp  $b$  the conjugate momentum. Then this equation can also be rewritten as [3]

$$v_{\tau\tau} = -\frac{\partial}{\partial v} V_{\text{eff}}(v), \quad (13)$$

where

$$V_{\text{eff}}(v) = \frac{1}{2v^2} + \frac{1}{2}v^2 - \frac{\sigma P}{3v^3}. \quad (14)$$

The dynamics of a condensate is different for the cases of positive and negative atomic scattering lengths. We will analyse these cases separately. First, for the sake of completeness, let us consider  $P_1 = 0$ , that is, the case when the scattering length is constant.

In realistic situations, the energy dissipation is present. The Gross–Pitaevskii equation in this case takes the form [24–27]

$$(i - \gamma)\hbar\Psi_t = -\frac{\hbar^2}{2m}\Delta\Psi + V_{\text{tr}}\Psi + g|\Psi|^2\Psi + i\gamma\mu\Psi, \quad (15)$$

where  $\gamma$  is the phenomenological dissipation constant which is to be determined experimentally. For small values of the dissipation constant in the first approximation, we can replace the constant norm  $N$  in variational equations by the time-dependent  $N(t)$ . The variation of  $N(t)$  due to dissipation can be calculated. In principle, the appearance of the stationary value of the width should be expected, when the energy of driven oscillations due to variations in the scattering length is compensated by the dissipation. This problem requires separate investigation.

### 2.1. Positive scattering length

When  $\sigma = -1$ , i.e.  $a_{s0} > 0$ , the equilibrium points  $v_0$  of equation (10) satisfy:

$$v_0^5 = v_0 + P_0. \quad (16)$$

This is a fifth-order algebraic polynomial problem that has only one positive real root. Its solution corresponds to a stable equilibrium point. When the interactions are strong,  $P_0 \gg 1$ , one can neglect the term  $v_0$  and obtain  $v_0^{(0)} = P_0^{1/5}$ . After substitution of  $v_0 = v_0^{(0)} + \delta$  into (16), we obtain

$$v_0 = \frac{5P_0}{5(P_0)^{4/5} - 1}. \quad (17)$$

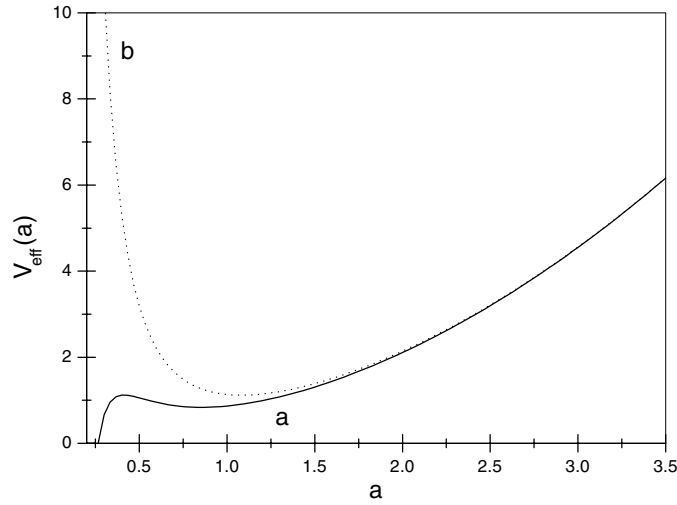


**Figure 1.** Effective potential used in describing the scaling parameter  $v$ . Two cases are presented: a,  $P_0 = 0.4$  (attractive BEC) and b,  $P_0 = -0.4$  (repulsive BEC).

This corresponds to the Thomas–Fermi regime, since we neglect the quantum pressure in comparison with parabolic potential and nonlinearity terms in the GP equation.

The frequency of small oscillations near this point is

$$\omega_r \approx \sqrt{5} \left( 1 + \frac{3}{10P_0^{4/5}} \right), \quad (18)$$

where it is assumed that  $P_0 \gg 1$ .

## 2.2. Negative scattering length

Typical behaviour of  $V_{\text{eff}}(v)$  for two cases, attractive and repulsive condensates, is presented in figure 1.

The equation for the equilibrium position

$$v_0 = \frac{1}{v_0^3} - \frac{P_0}{v_0^4}, \quad (16')$$

has either no, or two positive real solutions. The critical value of  $P_0$  is given by

$$P_c = \frac{4}{5^{5/4}} = 0.5350. \quad (19)$$

When  $P_0 > P_c$ , there are no equilibrium points, and the condensate will collapse. This value was obtained by many authors (see for example [28] and references therein and also [29]). When  $P_0 < P_c$  there are two equilibrium points, one of them unstable ( $v_{01}$ ) and the other stable ( $v_{02}$ ). This means that collapse can be avoided when two conditions are satisfied:

- (a)  $P_0 < P_c$
- (b) the initial condition:  $v_{03} > v > v_{01}$ , where  $v_{03}$  is defined by:  $V(v_{03}) = V(v_{01})$ .

In this region, the motion should be periodic motion around the equilibrium point.

When  $P_0 \ll 1$  for the equilibrium point of (10) (the minimum of the potential  $V_{\text{eff}}$ , see figure 1) we have the following approximation:

$$v_0 = 1 - \frac{P_0}{4}. \quad (20)$$

In the interval  $0 < P_0 < 0.5$ , the position of maximum of the potential function  $V_{\text{eff}}$  is well approximated by  $v_{01} \approx P_0$ , the point  $v_{03} \approx 1/(\sqrt{3}P_0)$ . The frequency of small oscillations near  $v_0$  is

$$\omega_a \approx 2\sqrt{1 - \frac{P_0}{4}}. \quad (21)$$

### 3. Periodic variation in scattering length

One of the problems of interest in BEC is the study of the oscillation in the condensate subject to a periodic variation of the scattering length [13, 17, 18, 11]. Such a variation, as mentioned above, can be achieved experimentally by varying the magnetic field or using optically induced Feshbach resonances. In the GP equation, the temporal modulation of the scattering length of atoms corresponds to a time-dependent nonlinear coefficient.

For the sinusoidal variations of the atomic scattering length (11), equation (10) takes the form:

$$\frac{d^2v}{d\tau^2} + v = \frac{1}{v^3} - \frac{\sigma P_0}{v^4} - \frac{\sigma P_1}{v^4} \sin(\Omega t). \quad (22)$$

We are looking for a solution of this equation in the form

$$v = v_0 + v_1,$$

where  $v_1 \ll v_0$  is a small deviation from the equilibrium position  $v_0$ . Substituting it into (22) and expanding the terms of the equation near the equilibrium point  $v_0$  we get the equation for  $v_1$ :

$$\ddot{v}_1 + \omega_0^2 v_1 + A v_1^2 + B v_1^3 + \dots = (C + D v_1 + E v_1^2 + F v_1^3 + \dots) \sin(\Omega t). \quad (23)$$

Above, we introduced the following constants:

$$\begin{aligned} \omega_0^2 &= 1 + 3/v_0^4 - 4\frac{\sigma P_0}{v_0^5}, & A &= -6/v_0^5 + 10\sigma P_0/v_0^6, & B &= 10/v_0^6 - 20\sigma P_0/v_0^7, \\ C &= -\sigma P_1/v_0^4, & D &= 4\sigma P_1/v_0^5, & E &= -10\sigma P_1/v_0^6, & F &= 20\sigma P_1/v_0^7. \end{aligned}$$

In addition, we will assume that  $v_1$  and  $P_1$  are small quantities of the same order, say  $\varepsilon$ . (Note that constants  $C$ ,  $D$ ,  $E$  and  $F$  depend on  $P_1$ .) Then, we can keep in equation (23) terms up to order  $\varepsilon^3$ :

$$\ddot{v}_1 + \omega_0^2 v_1 + A v_1^2 + B v_1^3 = (C + D v_1 + E v_1^2) \sin(\Omega t). \quad (24)$$

Now, we proceed with the examination of the resonance cases of equation (24). We assume that

$$\omega_0 \approx \frac{p}{q}\Omega,$$

where  $p$  and  $q$  are mutually prime integers. Solution of equation (24) may be sought in the form of the expansion

$$v_1 = a \cos(\Omega t + \theta) + h x^{(1)} + h^2 x^{(2)} + \dots, \quad (25)$$

where  $h$  is the amplitude of periodical perturbation (see equation (2)). Making use of the successive approximation method described in [30], in the case of a *main resonance* ( $p = q = 1$ ) we get the following set of equations for the amplitude  $a$  and phase  $\theta$ :

$$\frac{da}{dt} = \left( -\frac{C}{2\Omega} - \frac{E}{8\Omega}a^2 \right) \cos \theta, \quad (26)$$

$$\frac{d\theta}{dt} = \omega_0 - \Omega + \frac{C}{2a\Omega} \sin \theta + \left( \frac{3B}{8\Omega} - \frac{5A^2}{12\omega_0^2\Omega} \right) a^2 + \frac{3E}{8\Omega}a \sin \theta. \quad (26')$$

For the steady-state regime  $da/dt = d\theta/dt = 0$ . Then the amplitude frequency response can be easily found:

$$\beta a^3 \pm 3Ea^2 \pm 4C + 8\Omega\gamma a = 0, \quad (27)$$

where  $\gamma = \omega_0 - \Omega$ ,  $|\gamma| \ll 1$  and

$$\beta = 3B - \frac{10A^2}{3\omega_0^2}. \quad (27')$$

The signs ( $\pm$ ) in (27) correspond to different branches of the response (e.g. see figure 6).

System (26) can be transformed into Hamiltonian form by changing the variable  $a = \sqrt{Q}$ . In this case  $dQ/dt = \partial H/\partial \theta$  and  $d\theta/dt = -\partial H/\partial Q$ , where

$$H(Q, \theta) = -\frac{C}{\Omega}\sqrt{Q} \sin \theta - \frac{E}{4\Omega}Q^{3/2} \sin \theta + (\Omega - \omega_0)Q - \frac{\beta}{16\Omega}Q^2. \quad (28)$$

In the case of *parametric resonance* ( $p = 1, q = 2, v_1 = a \cos(\frac{1}{2}\Omega t + \theta)$ ), the equations for  $a$  and  $\theta$  have the form:

$$\frac{da}{dt} = -\frac{D}{2\Omega}a \cos(2\theta) \quad (29)$$

$$\frac{d\theta}{dt} = \omega_0 - \frac{1}{2}\Omega + \frac{D}{2\Omega} \sin(2\theta) + \left( \frac{3B}{4\Omega} - \frac{5A^2}{6\omega_0^2\Omega} \right) a^2. \quad (30)$$

The corresponding Hamiltonian is

$$H_p(Q, \theta) = -\frac{D}{2\Omega}Q \sin(2\theta) + \left( \frac{1}{2}\Omega - \omega_0 \right) Q - \frac{\beta}{8\Omega}Q^2. \quad (31)$$

It follows that  $H$  is the integral of motion and there exists a separatrix  $H = 0$  separating finite trajectories corresponding to nonlinear resonances from infinite ones.

Phase planes for two cases of attractive BEC ( $\sigma = 1$ ) with  $P_0 = 0.2$  and  $P_0 = 0.4$  are shown in figure 2. As seen, the portraits differ drastically. The reason is different signs of factor  $\beta$  entering equation (26) for the cases  $P_0 = 0.2$  and  $P_0 = 0.4$ .

Phase planes for two cases of repulsive BEC ( $\sigma = -1$ ) with  $P_0 = 0.4$  and  $P_0 = 0.8$  are shown in figure 3.

### 3.1. Dynamics of an attractive condensate under periodic $a_s$

Oscillations with the maximum amplitude for the case of the main resonance take place for separatrix  $H_s \approx 0$  when  $\theta = \pi/2$  (see equation (28)). The critical drive amplitude  $P_{1c}$  providing the maximum amplitude of the attractive condensate width oscillations,  $a_{\max}$  may be obtained from (27). In order to obtain an expression for  $P_{1c}$  let us rewrite the above-defined

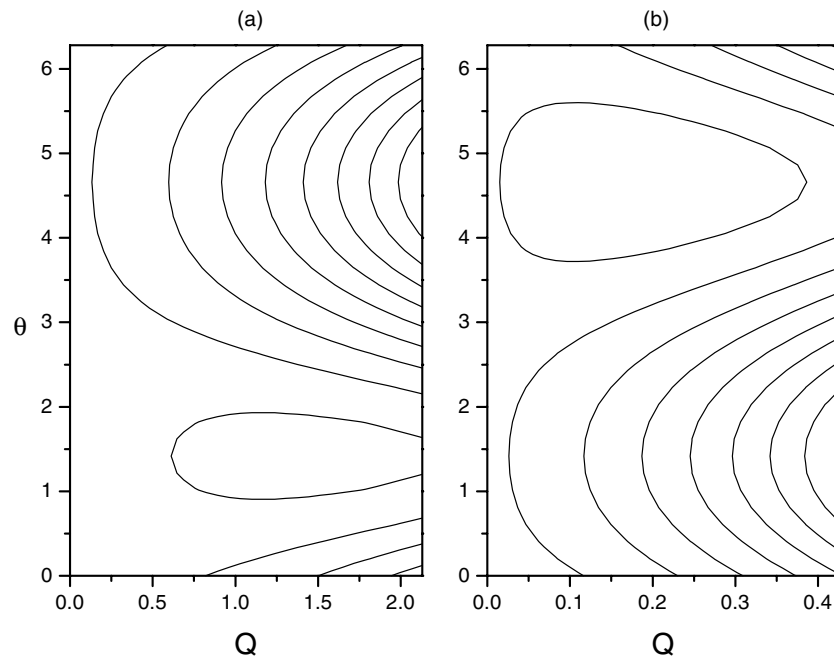


**Figure 2.** The phase planes for the system (26), (26') at (a)  $P_0 = 0.2$  ( $P_1 = 0.008$ ,  $\Omega = 1.936$ ) and (b)  $P_0 = 0.4$  ( $P_1 = 0.016$ ,  $\Omega = 1.766$ ) for  $\sigma = 1$  (attractive BEC),  $\gamma = 0$  and different  $H$ .

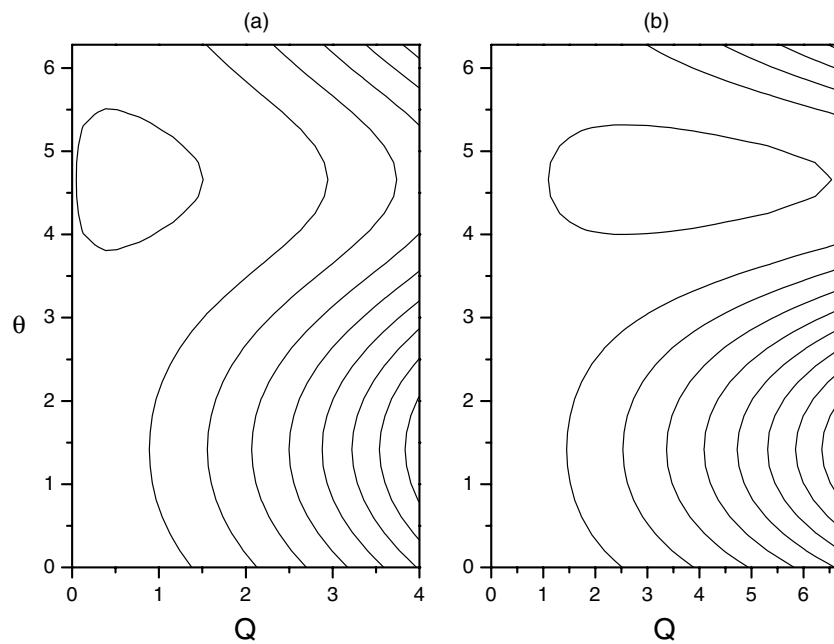


**Figure 3.** The phase planes for the system (26), (26') at (a)  $P_0 = 0.4$  ( $P_1 = 0.06$ ,  $\Omega = 2.066$ ) and (b)  $P_0 = 0.8$  ( $P_1 = 0.2$ ,  $\Omega = 2.100$ ) for  $\sigma = -1$  (repulsive BEC),  $\gamma = 0$  and different  $H$ .

parameters  $C$ ,  $D$  and  $E$  introducing new ones  $c$ ,  $d$ ,  $e$  as  $C = P_1 c$ ,  $D = P_1 d$  and  $E = P_1 e$ . Then in the case of  $\Omega = \omega_0$  ( $\gamma = 0$ ) we get

$$P_{1c} = \frac{|\beta| a_{\max}^2}{\left| 3e a_{\max} + \frac{4c}{a_{\max}} \right|}. \quad (32)$$

The maximum amplitude  $a_{\max}$  is found as follows. As is known the particle leaves the well (14) when its kinetic energy  $\langle v_{1t}^2 \rangle / 2$  becomes comparable with the difference between the potential well bottom and separatrix,  $\Delta V$ . This energy is

$$\Delta V = V_{\text{eff}}(v_{01}) - V_{\text{eff}}(v_0), \quad (33)$$

where  $v_0$  is a stable and  $v_{01}$  is an unstable equilibrium point (see subsection 2.2). For the case of slowly varying amplitude  $a$  and phase  $\theta$ , we have from equation (25):

$$v_{1t} = -a\Omega \sin(\Omega t + \theta). \quad (34)$$

Equating the critical value of the kinetical energy corresponding to the maximum amplitude of oscillations  $a_{\max}$  with  $\Delta V$ , we arrive at the following expression:

$$a_{\max} = \frac{\sqrt{2\Delta V}}{\Omega}. \quad (35)$$

Another way of calculating the maximum amplitude,  $a_{\max}$ , is to employ a direct expression for it

$$a_{\max} = \frac{1}{2}(v_{03} - v_{01}), \quad (36)$$

where the points  $v_{03}$  and  $v_{01}$  have been defined in subsection 2.2.

In the region  $0 < P_0 < 0.4$  where the well is deep, we have the approximations  $v_{01} \approx P_0$  and  $v_{03} \approx \frac{1}{\sqrt{3}P_0} - \frac{9}{2\sqrt{3}}P_0^3$ . Then in the indicated region of  $P_0$  for  $a_{\max}$  we get a very good approximation

$$a_{\max} \approx \frac{1}{2} \left( \frac{1}{\sqrt{3}P_0} - \frac{9}{2\sqrt{3}}P_0^3 - P_0 \right). \quad (37)$$

#### 4. The results of numerical simulations of the full Gross–Pitaevskii equation

Based on the above-stated theory, we can now proceed to numerical simulations to test calculations of the previous sections and carry out more detailed analysis. We discretize the problem in a standard way, with time step  $\Delta\tau$  and spatial step  $\Delta r$ , so  $U_j^k$  approximates  $U(j\Delta r, k\Delta\tau)$ . More specifically we approximate the governing equation (5) with the following second-order accurate semi-implicit Crank–Nicholson scheme,

$$\begin{aligned} \frac{i(U_j^{k+1} - U_j^k)}{\Delta\tau} &= -\frac{1}{2\Delta r^2} [(U_{j-1}^{k+1} - 2U_j^{k+1} + U_{j+1}^{k+1}) + (U_{j-1}^k - 2U_j^k + U_{j+1}^k)] \\ &\quad - \frac{1}{2r_j\Delta r} [(U_{j+1}^{k+1} - U_{j-1}^{k+1}) + (U_{j+1}^k - U_{j-1}^k)] \\ &\quad + \frac{1}{2} \left[ \frac{r_j^2}{2} (1 + h \sin(\Omega\tau_k)) \sigma |U_j^k|^2 \right] (U_j^k + U_j^{k+1}). \end{aligned} \quad (38)$$

The set of algebraic equations (38) is solved by the vectorial sweep method.

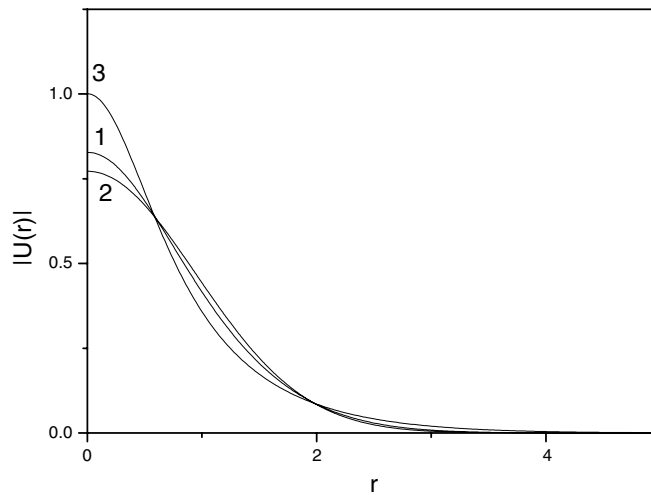


**Figure 4.** Profile of initial wave packets  $|U(\rho, \tau = 0)|$  corresponding to ansätze 1, 2 and 3. The parameters of the wave packets are chosen to give the same value of the system parameter  $P_0 = 0.2$ .

In solving the full governing partial differential equation (PDE) (5) both for attractive BEC ( $\sigma = +1$ ) and repulsive BEC ( $\sigma = -1$ ), we employ three different ansätze as initial wave packets: ansatz 1, called a Gaussian one [31, 32, 2], with the trial function in (7) chosen as

$$R\left(\frac{\rho}{a}\right) = \exp\left(-\frac{1}{2}\left(\frac{\rho}{a}\right)^2\right),$$

and ansätze 2 and 3 when the trial function  $R\left(\frac{\rho}{a}\right) = R(\xi)$  where  $R(\xi)$  is the solution of the equation

$$\frac{1}{2} \frac{d^2 R}{d\xi^2} + \frac{1}{\xi} \frac{dR}{d\xi} - \frac{\xi^2}{2} R + R^3 - \lambda R = 0 \quad (39)$$

with  $\lambda$  equal to  $-1$  and  $+1$  correspondingly. Such a choice enables us to use different initial wave packets.

The parameters of the initial wave packet are chosen to provide the given value of the norm  $N$  and  $P_0$  determined by equations (12) and (11).

In PDE simulations, the current values of the scaling parameter  $a(\tau)$  are calculated as follows:

$$a(\tau) = a_0 \sqrt{\frac{\int d\rho \rho^4 |U(\rho, \tau)|^2}{\int d\rho \rho^4 |U(\rho, 0)|^2}}. \quad (40)$$

Figure 4 depicts the profile of initial wave packets  $|U(\rho, \tau = 0)|$  corresponding to ansätze 1, 2 and 3. Parameters of the wave packets are chosen to give the same value of the system parameter  $P_0 = 0.2$ .

The main wave packet parameters are given in the table below.

Wave packet	Norm $N$	$\langle r \rangle$
Ansatz 1	0.019 73	1.062 50
Ansatz 2	0.022 54	1.070 56
Ansatz 3	0.018 36	1.066 98

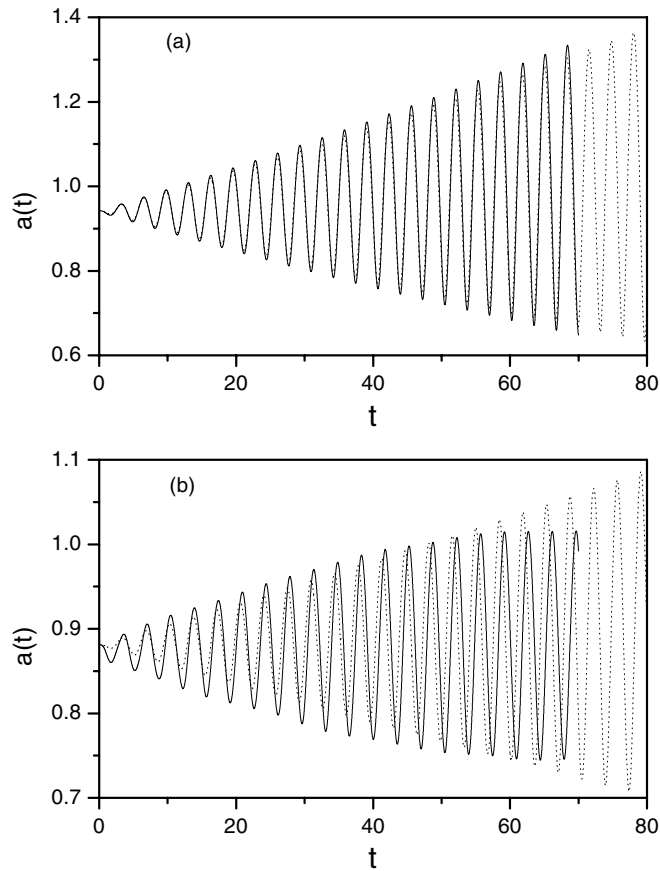


**Figure 5.** Dynamics of the scaling parameter  $a$  of an attractive BEC under main resonance ( $\Omega = \omega_0$ ) obtained from PDE and ODE calculations, (a)  $P_0 = 0.2$ ,  $P_1 = 0.014$  and (b)  $P_0 = 0.35$ ,  $P_1 = 0.00525$ . The solid line is for PDE and the dotted line is for ODE calculations. In both PDE simulations the initial wave packets are Gaussian.

As will be seen further in spite of some differences in the wave packet parameters, their dynamics are almost identical at small values of  $P_0$ . It should also be noted that ansatz 1 gives the exact solution at  $P_0 = 0$ , ansatz 2 does it at  $P_0 = 0.372$  and ansatz 3 corresponds to a collapsing solution.

#### 4.1. Attractive condensate ( $\sigma = +1$ )

The results of numerical simulations of PDE and ODE models in the case of the *main resonance* are presented below.

Figure 5 depicts dynamics of the scaling parameter  $a$  of an attractive BEC under the main resonance obtained from PDE and ODE calculations for two cases with: (a)  $P_0 = 0.2$ ,  $P_1 = 0.014$  and (b)  $P_0 = 0.35$ ,  $P_1 = 0.00525$ . The frequency  $\Omega$  of the periodical perturbation is taken to be equal to the eigenfrequency of the system  $\omega_0$  determined by

$$\omega_a = 2\sqrt{1 - \frac{P_0}{4v_0^5}}. \quad (41)$$

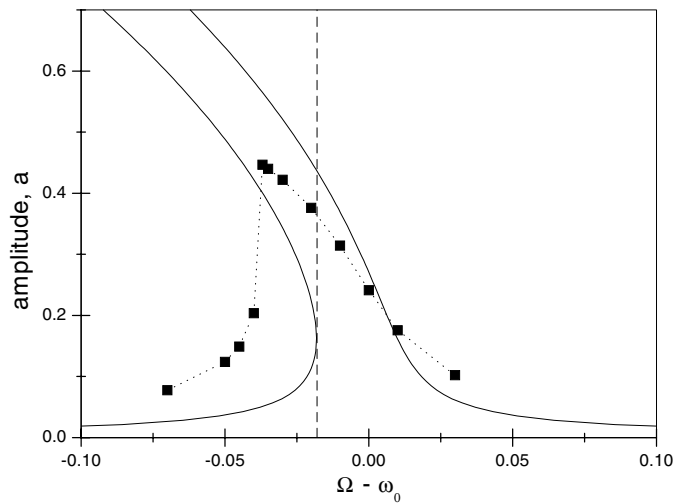


**Figure 6.** Amplitude frequency responses obtained from full PDE simulations (dotted line) and from theory (solid line) for the case when  $P_0 = 0.372$ ,  $P_1 = 0.00372$  and  $\sigma = 1$  (attractive BEC). In PDE calculations, ansatz 2 from equation (27) is used as the initial wave packet.

In both cases of PDE simulations, the initial wave packet has Gaussian form. The agreement between simulations of the full PDE and ODE in case (a) is good enough for times less than 100. In case (b) when  $P_0 = 0.35$  there is clearly some discrepancy in the actual value of oscillation amplitude. It may be explained by the shift of the equilibrium point in full PDE calculations.

In the case of the *main resonance*, the amplitude frequency response of the scaling parameter resonant oscillations is described by equation (27). The theoretical amplitude frequency response based on this equation and the one obtained from full PDE simulations for the case of  $P_0 = 0.3$  and  $P_1 = 0.0045$  are given in figure 6. In PDE calculations, a self-similar ansatz (ansatz 2) from equation (27) is used as the initial wave packet. Each point of the plot results from PDE simulation of the scaling parameter evolution under the main resonance starting from the stationary point  $a_0$  where the oscillation amplitude is equal to zero.

The factor  $\beta$  in (27) plays an important role in the amplitude frequency response. Its sign determines the incline direction in the plot of the response and its value determines the degree of the nonlinearity in the main resonance. Small values of the factor  $\beta$  mean prevalence of the linear regime in the resonance.

As shown above, collapse of the attractive BEC condensate can be avoided when  $P_0 < P_c$  (see (19)). We have carried out full PDE simulations to study conditions when the main resonance makes the BEC leave the potential well  $V_{\text{eff}}$  and the BEC begins to collapse. In terms of the effective Hamiltonian (28) this means that when in the resonance the amplitude of oscillations exceeds the value on the separatrix ( $H > 0$ ), the condensate collapses.

The dependence of the critical drive amplitude  $P_{1c}$  on  $P_0$  obtained from ODE (solid line) and PDE (filled squares) numerical simulations as well as the theoretical dependence (32) (dotted line) is shown in figure 7. The theoretical curve is obtained from equation (32) using approximation (37) at  $0 < P_0 < 0.4$  and expression (35) at  $0.4 \geq P_0 < P_{1c}$ . As seen, ODE simulations based on equation (22) are in good agreement with PDE simulations of the full Gross–Pitaevskii equation (5) where self-similar ansatz 2 ( $\lambda = -1$ ) is used as an initial wave packet.

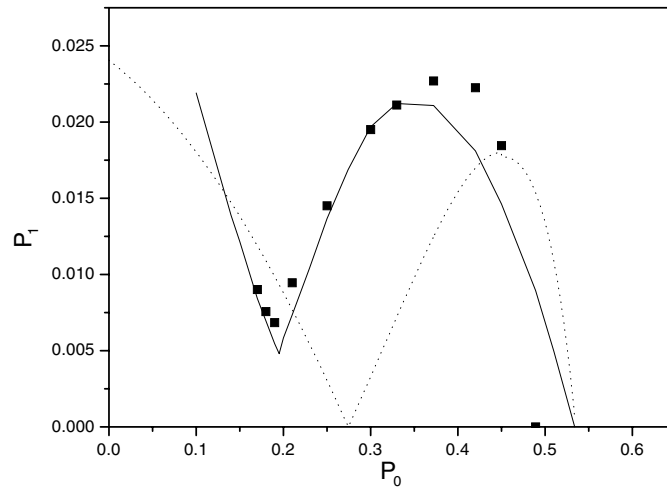


**Figure 7.** Dependence of the critical drive  $P_{1c}$  leading to collapse on  $P_0$ . The solid line is for ODE calculations and the filled squares are for full PDE calculations. The self-similar ansatz (ansatz 2) with  $\lambda = -1$  is chosen for the initial wave packet in PDE simulations. The theoretical dependence (32) is shown by the dotted line.

The dependences obtained from ODE and PDE simulations have a brightly expressed minimum at the point  $P_0 = 0.2$ . It may be explained by the supposition that the *resonance* at this point is mainly linear. Indeed in accordance with equation (27') the factor  $\beta$  entering the formula for the amplitude–frequency response goes to zero at  $P_0 \approx 0.277$ . It means that at this point the resonance is close to linear and a small value of external drive  $P_1$  leads to large amplitudes of the BEC oscillations. Discrepancy between the position of the minimum in the theoretical curve and that obtained from numerical simulations may be explained by the fact that in deriving the governing equation (23), the terms of degree higher than 3 are not taken into account.

The next plot in figure 8 depicts the dynamics of the *parametric* resonance ( $\Omega = 2\omega_0$ ) at the point  $P_0 = 0.36$  when  $P_1 = 0.051$ . Full PDE calculations were carried out with the initial wave packet corresponding to ansatz 3 ( $\lambda = 1$ ).

As seen at times  $t < 50$  parametric resonance is proved to be suppressed in accordance with the prediction of the theory.

#### 4.2. Repulsive condensate ( $\sigma = -1$ )

The dynamics of the scaling parameter  $a$  of a repulsive condensate under the main resonance obtained from PDE and ODE calculations for the case  $P_0 = 0.4$ ,  $P_1 = 0.06$  is shown in figure 9. The frequency of the periodical perturbation  $\Omega = \omega_0$ , where the eigenfrequency  $\omega_0$  is determined as

$$\omega_a = 2\sqrt{1 + \frac{P_0}{4v_0^5}} \quad (42)$$

(for comparison see equation (41)). The initial wave packet has Gaussian form (ansatz 1).

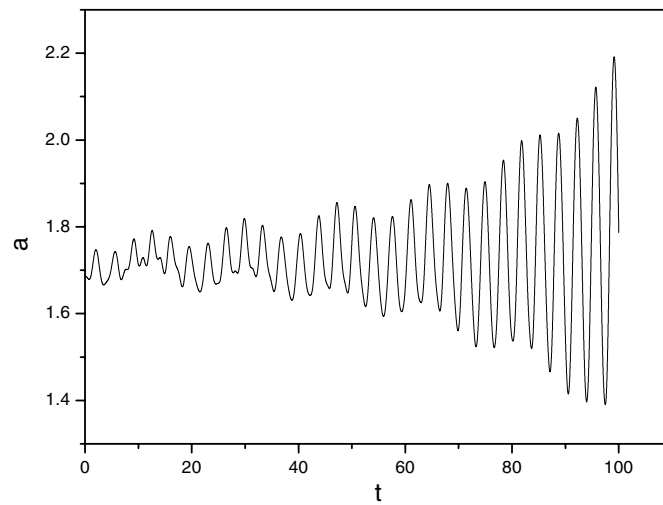


**Figure 8.** Dynamics of the scaling parameter  $a$  under *parametric resonance* ( $\Omega = 2\omega_0$ ) obtained from full PDE calculations for  $P_0 = 0.36$  and  $P_1 = 0.051$ . As the initial wave packet self-similar ansatz 3 ( $\lambda = 1$ ) is used.

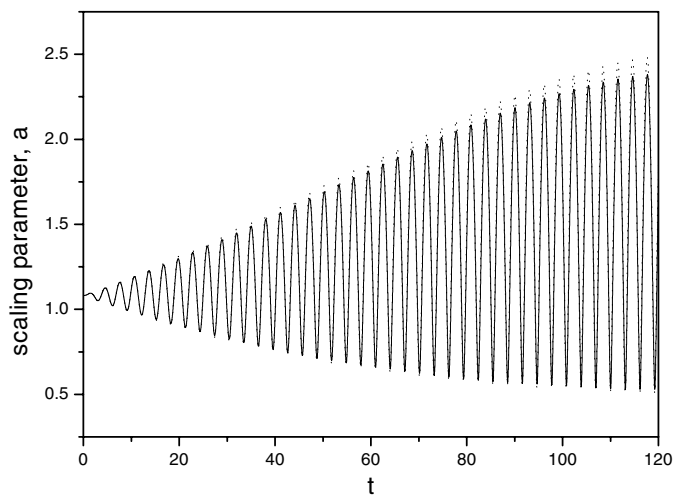


**Figure 9.** Dynamics of the scaling parameter  $a$  of a repulsive BEC under the main resonance ( $\Omega = \omega_0$ ) obtained from PDE and ODE calculations,  $P_0 = 0.4$ ,  $P_1 = 0.06$  ( $\omega_0 = 2.0664$ ). The solid line is for PDE and the dotted line is for ODE calculations. The initial wave packet is chosen to be Gaussian.

The agreement between simulations of the full PDE and ODE is excellent for times less than 100.

The dynamics of the repulsive BEC under *parametric resonance* ( $\Omega = 2\omega_0$ ) obtained from full PDE calculations for  $P_0 = 0.4$  and  $P_1 = 0.12$  are shown in figure 10. Two cases are presented, the case when the initial wave packet: (a) has self-similar form (39) with  $\lambda = 1$  (ansatz 3) and (b) is Gaussian (ansatz 3).

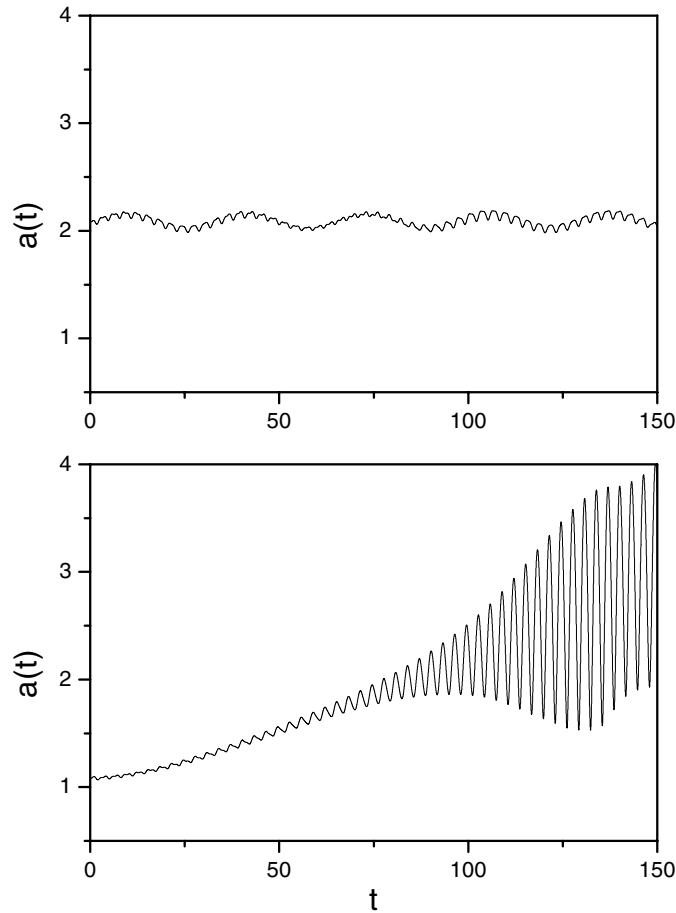


**Figure 10.** Dynamics of the repulsive BEC under *parametric resonance* ( $\Omega = 2\omega_0$ ) obtained from full PDE calculations when  $P_0 = 0.4$  and  $P_1 = 0.12$ . Two cases are presented: (a) when self-similar ansatz 3 is used as the initial wave packet and (b) when the initial wave packet is Gaussian.

## 5. Conclusion

In this work, we study the nonlinear oscillations of the 3D spherical symmetric Bose–Einstein condensate under periodic variation in time of the atomic scattering length. We employ the time-dependent variational approach and derive the equation for the dynamics of the condensate width. The equation has the form of the anharmonic oscillator under the singular periodic drive. Using this equation, we analyse analytically the resonance characteristics for the cases of attractive and repulsive condensates.

In particular, we investigate the process of the attractive condensate collapse with  $N < N_c$  under periodic variations of the scattering length. We find the possibility of bistability in the oscillations' condensate width depending on the detuning between the drive frequency and the frequency of small oscillations of a condensate.

We have shown that even when the number of the condensate atoms is less than critical, the condensate can collapse. Using the variational approach equation, we derive the dependence of the driving force critical value  $P_{1c}$  versus initial parameter  $P_0$ .

For the repulsive condensate case, we study both main and parametric resonances in condensate oscillations. The full numerical simulations of the Gross–Pitaevskii equation with periodic nonlinear coefficient confirm predictions on the basis of the variational approach. We find the deviations from predictions of the variational approach for the case when the number of atoms is close to the critical one.

### Acknowledgments

We acknowledge partial support by the FAPESP, Brazil.

### References

- [1] Dalfovo F, Giorgini S, Pitaevskii L P and Stringari S 1999 *Rev. Mod. Phys.* **71** 463
- [2] Garcia V M *et al* 1999 *Phys. Rev. Lett.* **83** 1715
- [3] Perez-Garcia V M *et al* 1997 *Phys. Rev. A* **56** 1424  
Perez-Garcia V M *et al* 1999 *Phys. Rev. A* **59** 2220
- [4] Stringari S 1996 *Phys. Rev. Lett.* **77** 2360
- [5] Castin Y and Dum R 1998 *Phys. Rev. Lett.* **79** 3553
- [6] Abdullaev F Kh and Galimzyanov R M 2003 *J. Phys. B: At. Mol. Opt. Phys.* **36** 1099
- [7] Jin D S *et al* 1996 *Phys. Rev. Lett.* **77** 420  
Mewes M O *et al* 1996 *Phys. Rev. Lett.* **77** 988
- [8] Garnier J, Abdullaev F Kh and Baizakov B B 2004 *Phys. Rev. A* **69** 053607
- [9] Kagan Yu, Surkov E L and Shlyapnikov G V 1996 *Phys. Rev. Lett.* **79** 2604
- [10] Cornish S L *et al* 2000 *Phys. Rev. Lett.* **85** 1795
- [11] Staliunas K, Longhi S and Valcárcel G J 2002 *Phys. Rev. Lett.* **89** 210406
- [12] Abdullaev F Kh, Darmanyan S A, Bishoff S and Soerensen M P 1997 *J. Opt. Soc. Am. B* **14** 27
- [13] Abdullaev F Kh and Kraenkel R A 2000 *Phys. Lett. A* **292** 395
- [14] Saito H and Ueda M 2003 *Phys. Rev. Lett.* **90** 040403
- [15] Abdullaev F Kh, Caputo J G, Kraenkel R A and Malomed B A 2003 *Phys. Rev. A* **67** 013605
- [16] Abdullaev F Kh and Garnier J 2004 *Phys. Rev. A* submitted
- [17] Abdullaev F Kh, Bronski J and Galimzyanov R M 2003 *Physica D* **184** 319
- [18] Adhikari S K 2003 *J. Phys. B: At. Mol. Opt. Phys.* **36** 1109
- [19] Roberts J L *et al* 2001 *Phys. Rev. Lett.* **86** 4211
- [20] Kevrekidis P G, Theocharis G, Frantzeskakis D J and Malomed B A 2003 *Phys. Rev. Lett.* **90** 230401
- [21] Inouye S *et al* 1998 *Nature* **392** 151
- [22] Strecker K E *et al* 2002 *Nature* **417** 150
- [23] Courteille Ph W *et al* 1998 *Phys. Rev. Lett.* **81** 69
- [24] Choi S, Morgan S A and Burnett K 1998 *Phys. Rev. A* **57** 4057
- [25] Tsubota M, Kasamatsu K and Ueda M 2002 *Phys. Rev. A* **65** 023603
- [26] Adhikari S K 2004 *Phys. Rev. A* **69** 063613
- [27] Saito H and Ueda M 2004 *LANL Preprint* cond-mat/0407095
- [28] Kim Y E and Zubarev A L 1998 *Phys. Lett. A* **246** 389
- [29] Saito H and Ueda M 2001 *Phys. Rev. A* **63** 043601
- [30] Bogoliubov N N and Mitropolsky Y A 1961 *Asymptotic Methods in the Theory of Non-Linear Oscillation* (Delhi: Hindustan P. Corp.)
- [31] Anderson D, Lisak M and Reichel T 1988 *J. Opt. Soc. Am.* **5** 207
- [32] Stoof H T C 1997 *J. Stat. Phys.* **87** 1353